

Ultrafast dynamics in topological insulators

C. W. Luo*^a, H.-J. Chen^a, H. J. Wang^a, S. A. Ku^a, K. H. Wu^a, T. M. Uen^a, J. Y. Juang^a, J.-Y. Lin^b, B. L. Young^a, T. Kobayashi^a, R. Sankar^c, F. C. Chou^c, H. Berger^d, G. D. Gu^e

^a Department of Electrophysics, National Chiao Tung University, Hsinchu 300, Taiwan; ^b Institute of Physics, National Chiao Tung University, Hsinchu 300, Taiwan; ^c Center for Condensed Matter Sciences, National Taiwan University, Taipei 106, Taiwan; ^d Institute of Physics of Complex Matter, EPFL, 1015 Lausanne, Switzerland; ^e Condensed Matter Physics & Materials Science Department, Brookhaven National Laboratory, Upton, New York 11973, USA

*cwluo@g2.nctu.edu.tw; phone +886-3-5712121ext.56196; fax +886-3-5725230

ABSTRACT

Ultrafast dynamics of carriers and phonons in topological insulators $\text{Cu}_x\text{Bi}_2\text{Se}_{3-y}$ ($x=0, 0.1, 0.125, y=0, 1$) was studied using femtosecond optical pump-probe spectroscopy. One damped oscillation was clearly observed in the transient reflectivity changes ($\Delta R/R$), which is assigned to the coherent optical phonon (A_{1g}^1). According to the red shift of A_{1g}^1 phonon frequency, the Cu atoms in $\text{Cu}_x\text{Bi}_2\text{Se}_3$ crystals may predominantly intercalated between pair of the quintuple layers. Moreover, the carrier dynamics in the Dirac-cone surface state is significantly different from that in bulk state, which was investigated using optical pump mid-infrared (mid-IR) probe spectroscopy. The rising time and decay time of the negative component in $\Delta R/R$, which is assigned to carrier relaxation in Dirac cone, is 1.62 ps and 20.5 ps, respectively.

Keywords: Ultrafast dynamics, topological insulators, pump-probe spectroscopy

1. INTRODUCTION

The discovery of 3D topological insulators (TIs) initiated a new era of condensed matter physics¹⁻³. The gapless surface electronic states (Dirac fermions), caused by strong spin-orbit interactions, and the characterizations of their fundamental properties have been studied by various means, e.g. angle-resolved photoemission spectroscopy (ARPES)⁴⁻⁶ and scanning tunneling microscopy (STM)⁷⁻¹⁰, and the transport measurements¹¹⁻¹⁴. The special properties provide innovative opportunities for potentially revolutionary applications such as THz optoelectronics, spintronics, and quantum computation. Recently, the elements of Cu, Mn, Co, Fe, and Cr were doped into TIs to induce superconductivity¹⁵, ferromagnetism^{16,17}, and anomalous quantized Hall effect¹⁸. Thus, this kind of doping provides an important means to modify the surface electronic states of TIs, such as opening up a gap at the Dirac point¹⁹ and shifting the Fermi level⁵. However, the locations and role of these doped atoms in TIs remain elusive and are yet to be studied. For instance, a Bi_2Se_3 crystal is constructed by the repeated quintuple layers (QLs, including a sequence of Se(1)-Bi-Se(2)-Bi-Se(1) atoms) along *c*-axis and bonded to each other through van der Waals force. This specific property makes the layered compound Bi_2Se_3 crystals can be substituted and intercalated by a small percentage of doping atoms. For the similar case of Bi-rich Bi-Se compound, Bi_2Se_2 , a Bi-Bi slab is inserted between two QLs²⁰. That is, the additional Bi atoms are intercalated into the Bi_2Se_3 matrix to form the Bi_2 layers and simultaneously change the bond length and bond angle of QL through the extra Coulomb force from the doped atoms. Consequently, the characteristics of QL vibrations, corresponding to some specific phonon mode, in Bi-Se compound will be changed due to the doping. Ultrafast time-resolved pump-probe spectroscopy has been established as a protocol to study the phonon dynamics^{21,22} and is therefore employed in this work to gain insight into such critical changes of crystal structure with substitution or intercalation. In the present study, we use femtosecond optical pump-probe spectroscopy to investigate the dynamics of coherent optical phonons (COPs) in $\text{Cu}_x\text{Bi}_2\text{Se}_{3-y}$ ($x = 0, 0.1, 0.125, y=0, 1$) single crystals. From the frequency shifts and lifetime of the COPs, the locations of the Cu atoms in $\text{Cu}_x\text{Bi}_2\text{Se}_3$ can be determined, and the influence of the Cu atoms in QL is subsequently discussed.

Moreover, a wide range of photonic applications based on TIs, including thermal detection, high-speed optical communications, terahertz detection, image, and spectroscopy, are proposed recently. As the Dirac-cone surface state will play a crucial role in determining performances of any real TI devices, their better understanding in the individual

properties of bulk state and surface state, and their coupling mechanisms is imperative. Owing to the fact that the surface signatures are easily overwhelmed by bulk contributions, however, the most present experiments cannot directly separate the bulk and surface signals, which intimately couple together, in TIs. The recent time- and angle-resolved photoemission spectroscopy (TrARPES) studies have shown that the surface carrier population in TIs can be induced by photoexcitation²³, and separately obtained the temperature and chemical potential relaxation of surface and bulk²⁴. As well known, the ARPES is baffled by the surface issue. Therefore, we need a novel solution that is insensitive to the sample surface and can probe the bulk and surface states individually. Here we take the advantage of optical pump mid-infrared (mid-IR) probe spectroscopy, which is the bulk sensitive technique, to explore the nonequilibrium dynamics of TIs. The femtosecond-time resolution allows us to probe the fundamental relaxation processes directly within the conduction band and Dirac cone, and thus distinguish the separate dynamics in bulk and surface states.

2. EXPERIMENTS

2.1 Sample preparation

The single crystals of $\text{Cu}_x\text{Bi}_2\text{Se}_3$ ($x=0, 0.1, 0.125$) used in this study were grown using the following methods: vertical Bridgman and modified floating zone. Single crystals of $\text{Cu}_x\text{Bi}_2\text{Se}_3$ ($x=0, 0.1, 0.125$) and Bi_2Se_2 have been prepared using stoichiometric mixtures of 5N purity of Bi, Se, and Cu in sealed evacuated quartz tubes. The $\text{Cu}_x\text{Bi}_2\text{Se}_3$ crystals were grown with slow-cooling method from 850°C to 650°C at a rate of 2°C/h and then quenched in cold water. Single crystal Bi_2Se_2 has been prepared using vertical Bridgman method. Preliminary homogenization was carried out in a horizontal tube furnace at 350°C for 75 h. The sealed ampoules were then passed through a vertical Bridgman furnace between 650°C and 600°C of thermal gradient $\sim 1^\circ\text{C}/\text{cm}$ near the solidification point. The pulling rate was kept at 0.2 mm/h. The resulting crystals could be cleaved easily, and the freshly cleaved plane showed a silvery shining mirror-like surface. For the sample #2 of Bi_2Se_3 single crystal in Fig. 3, it was grown by a modified floating zone method, where the Se-rich Bi_2Se_3 was used in the melting zone. The Bi_2Se_3 material, of high-purity (99.9999%) Bi and Se, was pre-melted and loaded into a 10-mm diameter quartz tube. The crystal growth rate was controlled at 0.5 mm per hour. All of the samples were kept in a vacuum tank to avoid surface oxidation. Before each experiment, the sample was cleaved using a scotch tape to ensure that a flat and reflective surface was obtained.

2.2 Pump-probe spectroscopy

For the optical pump-probe measurements, the light source was provided by a commercial mode-locked Ti:sapphire laser system with the pulse duration of 100 fs, a repetition rate of 5 MHz, and a center wavelength of 800 nm. The fluences of the pump beam and the probe beam were 1 mJ/cm² and 0.067 mJ/cm², respectively. The pump beam was focused on the $\text{Cu}_x\text{Bi}_2\text{Se}_{3-y}$ single crystals with a diameter of 35 μm while the probe beam was focused on the center of the pump-beam spot with a diameter of 25 μm . The polarizations of pump and probe beams were orthogonal to each other; meanwhile, both were perpendicular to the c-axis of $\text{Cu}_x\text{Bi}_2\text{Se}_{3-y}$ single crystals. A linear motor stage was used to vary the delay time between the pump and probe pulses. The small transient reflectivity changes ($\Delta R/R$) of probe beam were detected by using a photodiode and a lock-in amplifier.

For the optical pump mid-infrared probe (OPMP) spectroscopy, a partial laser beam of the 800-nm Ti:sapphire regenerative amplifier with a repetition rate of 5 KHz and pulse duration of 30 fs was focused on the surface of the samples with a diameter of 500 μm . The pumping fluence was tuned by varying the laser output power. The remainder laser beam was used to generate mid-infrared pulses via the differential frequency generation (DFG) in a 0.7-mm-thick GaSe crystal. The ultrafast dynamics of TIs was studied by measuring the photoinduced transient reflectivity changes ($\Delta R/R$) of the probe beam with the photon energy of 141 meV.

3. ULTRAFAST PHONON DYNAMICS

Figure 1 displays the typical $\Delta R/R$ as a function of time delay in Bi_2Se_3 single crystals measured at room temperature. In general, the $\Delta R/R$ curve can be decomposed into several components corresponding to different energy-transfer processes, i.e. a fast component of a sub-picosecond time scale characterizes the thermalization between electrons and optical phonons and a subsequent slow component of several picoseconds represents the thermalization between

electrons and acoustic phonons²⁵. In addition, one damped oscillation component is superimposed on the $\Delta R/R$ curves as shown in the inset of Fig. 1. The frequency of this component is centered at 2.15 THz which has been assigned to the A_{1g}^1 coherent optical phonon (COP) mode²⁶ of Bi_2Se_3 (see Fig. 2). For the case of a Bi_2Se_2 crystal, two characteristic peaks centered at 2.03 THz and 3.32 THz are observed in Fig. 2, which are close to the A_{1g}^1 mode frequencies of the Bi and Bi_2Se_3 crystals, respectively. Nevertheless, both peaks slightly shift away from the characteristic frequencies of the A_{1g}^1 mode in pure Bi and Bi_2Se_3 crystals. These shifts of the spectral peaks can be explained by the changes in bond lengths due to the covalent bonding between the Se-Bi-Se-Bi-Se five-atom slab and the Bi-Bi two-atom slab in the Bi_2Se_2 crystals²⁰. Compared with the pure Bi and Bi_2Se_3 crystals, this additional covalent bonding would rearrange the length (or angle) of Bi-Bi bonds and Se-Bi-Se-Bi-Se chains in the Bi_2Se_2 crystals. The length of Se-Bi-Se-Bi-Se chain (one QL) stretches from 11.75 Å in a Bi_2Se_3 crystal to 11.80 Å in a Bi_2Se_2 crystal²⁰ such that the A_{1g}^1 mode frequency of the QL-layer structure decreases from 2.15 THz in a Bi_2Se_3 crystal to 2.03 THz in a Bi_2Se_2 crystal. On the contrary, the length of the Bi-Bi bond in Bi_2Se_2 shortens from 3.06 Å in a Bi crystal to 2.99 Å in a Bi_2Se_2 crystal²⁰ such that the A_{1g}^1 mode frequency of the Bi-Bi layer structure increases from 2.93 THz in a Bi crystal to 3.32 THz in a Bi_2Se_2 crystal. For the Se-Bi-Se-Bi-Se chain, the frequency shift is -0.12 THz corresponding to a 0.43% change in the chain length; meanwhile, for the Bi-Bi layers, the frequency shift is 0.39 THz corresponding to a -2.29% change in the bond length. These results indicate that in Bi_2Se_2 , where extra Bi atoms are intercalated between QLs, the phonon frequency of the A_{1g}^1 mode of the QL exhibits a red shift compared to that in Bi_2Se_3 . Furthermore, Yu et al.¹⁸ studied the rhombohedral V_2VI_3 compounds by Raman scattering spectroscopy and found a blue shift in the phonon frequency when the lighter Sb atoms exactly substitute Bi atoms in the QL of $Bi_{2-y}Sb_yTe_3$. Therefore, it appears that the microstructural deformation in the Bi_2Se_2 crystals can be unambiguously revealed by measuring the magnitude and sign of the phonon frequency shift of the QL.

As mentioned above, for the substitution case, i.e. a Bi atom is replaced by a doped atom, the phonon frequency of the A_{1g}^1 mode increases with increasing doping concentrations; while for the intercalation case, i.e. a doped atom is intercalated between two QLs, the phonon frequency of the A_{1g}^1 mode decreases with increasing doping concentrations. Therefore, the slightly red shift of A_{1g}^1 photon frequency as increasing Cu concentrations in the inset of Fig. 2 implies that the Cu atoms are intercalated in the $Cu_xBi_2Se_3$ crystals, which is consistent with the rise of the lattice constant of c-axis and the stretch of the QL chains. The stretch of the QL chains can be interpreted as follows, when the doping Cu atoms are intercalated between QLs, a mediated layer is formed to enhance the interaction between QLs and replaces the weak van der Waals interaction. Consequently, the length of a QL chains would be significantly stretched. Finally, the Cu atoms intercalated between every pair of QLs and cause an effective deformation in the QLs of $Cu_xBi_2Se_3$ crystals, which have been clearly revealed by the ultrafast phonon dynamics.

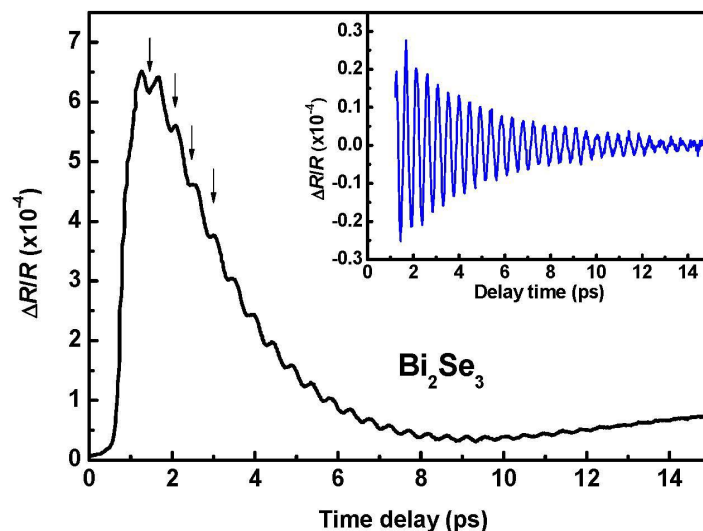


Figure 1. $\Delta R/R$ signals in a Bi_2Se_3 single crystal at room temperature. Inset: the oscillation component of $\Delta R/R$ signal in a Bi_2Se_3 crystal, which is extracted from the Fig. 1.

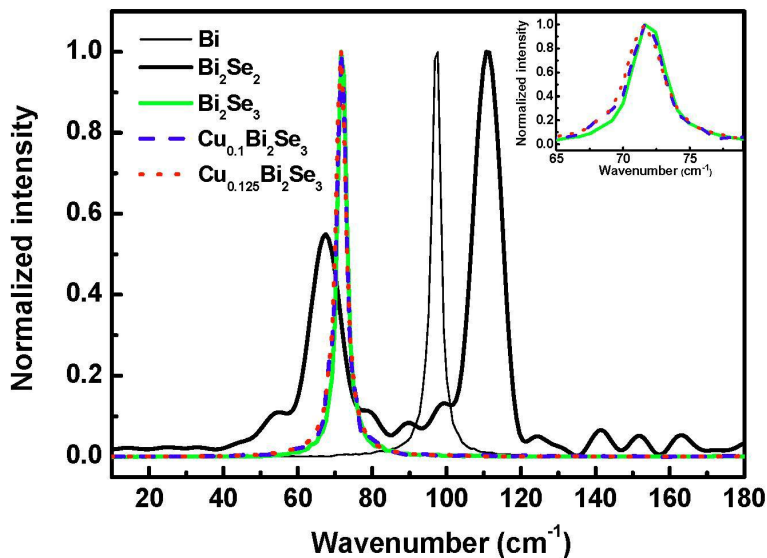


Figure 2. The Fourier transformation of the oscillation component of an $\Delta R/R$ signal in the inset of Fig. 1. Inset: the Fourier transformation of $\text{Cu}_x\text{Bi}_2\text{Se}_3$ crystals on an enlarged scale.

4. ULTRAFAST CARRIER DYNAMICS

Figure 3 is a typical OPMP spectra in Bi_2Se_3 with carrier concentration (n) of 51.5×10^{18} (Bi_2Se_3 #1) and 0.25×10^{18} (Bi_2Se_3 #2). For the case of Bi_2Se_3 #1, a positive peak is clearly observed in $\Delta R/R$. This positive peak gradually diminishes as the n decreases. Meanwhile, an additional negative peak appears at low carrier concentration, e.g. $n = 0.25 \times 10^{18}$, and its amplitude is inversely proportional to n . For the optical pumping and mid-IR probing processes, the probe photon energy (141 meV) of mid-IR used in this study is much smaller than the band gap of ~ 300 meV in Bi_2Se_3 , the interband transition between valence band (VB) and conduction band (CB) of bulk state does not happen. Thus, the interband absorption in CB and Dirac cone surface state will be the dominated processes after pumping, which are assigned to the positive and negative peaks in $\Delta R/R$, respectively. For the positive component in $\Delta R/R$, the excited carriers suffer the so-called intervalley scattering²⁷ to cause the red-shift of reflectance spectra after pumping. This result, consistent with the observations in n-type GaAs²⁷, reveals that the positive (or negative) signal within several ps timescale in $\Delta R/R$ is due to the mid-IR probe in bulk state of Bi_2Se_3 .

For the negative peak in $\Delta R/R$, we can obtain the rising time (τ_r) of 1.62 ps and decay time (τ_d) of 20.5 ps by fitting as shown in the inset of Fig. 3. Based on above dynamic information, we can further establish the ultrafast relaxation model for carriers in TIs. After pumping by the 1.55 eV photons, the major process is that the carriers in the bulk valence band (BVB) will be excited to band conduction band (BCB). However, owing to no unoccupied final density of states for the 1.55 eV pumping in the Dirac cone within bulk band gap, the carriers in Dirac cone cannot be excited. If the carrier recombination between the BCB and BVB is ignored, thus, the unoccupied states in BVB caused by pumping would be refilled through the bottom part of Dirac cone that almost overlaps with the top of BVB at the same momentum space. This implies that the carriers in Dirac cone can easily transfer into the unoccupied states in BVB and open an absorption channel for the mid-IR process in Dirac cone. Then, the reflectivity of mid-IR probing light will decrease within 1.62 ps, i.e. the rising time of negative peak in Fig. 3. Once the carriers in Dirac cone move out the Dirac cone, the BCB (like a carrier reservoir) subsequently injects the excited carriers into the unoccupied states in Dirac cone to close the absorption channel for the mid-IR process in Dirac cone and induce the increase of mid-IR reflectivity within 20.5 ps, which is consistent with the ARPES results²³ of a nonequilibrium population of the surface state persisting for >10 ps. This several tens of picoseconds in decay time, which is much longer than the rising time of several picoseconds, is due to the carriers in BCB cannot directly transfer into the top of Dirac cone without overlapping between them and other auxiliaries, e.g. phonons.

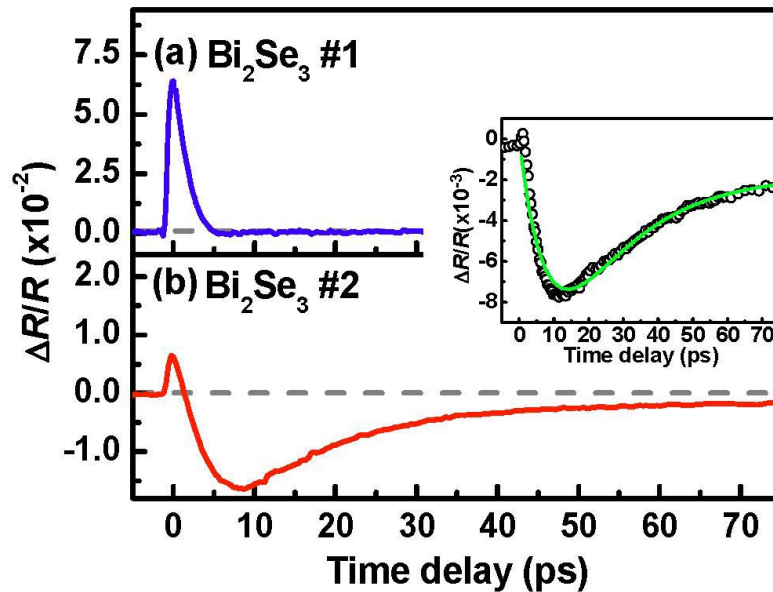


Figure 3. The carrier concentration (n) dependence of the transient changes in mid-infrared reflectivity $\Delta R/R$ of Bi_2Se_3 single crystals. (a) Sample #1 ($n=51.5 \times 10^{18}$) and (b) sample #2 ($n=0.25 \times 10^{18}$) were probed with photon energy of 141 meV. Inset: the negative component of $\Delta R/R$ in (b) was fitted by the exponential growth and decay functions.

5. SUMMARY

We have systematically studied the phonon dynamics in Bi, Bi_2Se_2 , and $\text{Cu}_x\text{Bi}_2\text{Se}_3$ ($x = 0, 0.1, 0.125$) single crystals using femtosecond pump-probe reflectivity spectroscopy. The frequency shifts of the phonon modes in Bi-rich Bi_2Se_2 crystals indicate that the extra Bi atoms are intercalated into the Bi_2Se_3 matrix and form a Bi_2 layer between the QLs. From the red shift of the A_{1g}^1 phonon frequency associated with the doping of Cu atoms, we also conclude that the additional Cu atoms are predominantly intercalated between QLs in $\text{Cu}_x\text{Bi}_2\text{Se}_3$ crystals. The studies of phonon dynamics in $\text{Cu}_x\text{Bi}_2\text{Se}_3$ crystals would provide the crucial information for understanding the superconductivity in topological insulators $\text{Cu}_x\text{Bi}_2\text{Se}_3$ crystals. Moreover, we utilized the ultrafast time-resolved spectroscopy with optical pump mid-infrared probe to explore the ultrafast dynamics of carriers in the surface state of TIs. The femtosecond-time resolution allows us to probe the fundamental relaxation processes directly within the conduction band and Dirac cone, and thus distinguish the individual dynamics in bulk and surface states.

6. ACKNOWLEDGMENTS

This project is financially sponsored by the National Science Council (grant no. NSC 98-2112-M-009-006-MY3, NSC 98-2112-M-009-008-MY3 and NSC 101-2112-M-009-016-MY2) and the Ministry of Education (MOE ATU program at NCTU) of Taiwan, R.O.C.

REFERENCES

- [1] Hsieh, D., Qian, D., Wray, L., Xia, Y., Hor, Y. S., Cava, R. J. and Hasan, M. Z., "A topological Dirac insulator in a quantum spin Hall phase," *Nature (London)* 452, 970-974 (2008).
- [2] Hasan, M. Z. and Kane, C. L., "Colloquium: Topological insulators," *Rev. Mod. Phys.* 82, 3045-3067 (2010).
- [3] Qi, X.-L. and Zhang, S.-C., "Topological insulators and superconductors," *Rev. Mod. Phys.* 83, 1057-1110 (2011).
- [4] Xia, Y., Qian, D., Hsieh, D., Wray, L., Pal, A., Lin, H., Bansil, A., Grauer, D., Hor, Y. S., Cava, R. J. and Hasan, M. Z., "Observation of a large-gap topological-insulator class with a single Dirac cone on the surface," *Nat. Phys.* 5, 398-402 (2009).
- [5] Hsieh, D., Xia, Y., Qian, D., Wray, L., Dil, J. H., Meier, F., Osterwalder, J., Patthey, L., Checkelsky, J. G., Ong, N. P., Fedorov, A. V., Lin, H., Bansil, A., Grauer, D., Hor, Y. S., Cava, R. J. and Hasan, M. Z., "A tunable topological insulator in the spin helical Dirac transport regime," *Nature (London)* 460, 1101-1106 (2009).
- [6] Chen, Y. L., Analytis, J. G., Chu, J.-H., Liu, Z. K., Mo, S.-K., Qi, X. L., Zhang, H. J., Lu, D. H., Dai, X., Fang, Z., Zhang, S. C., Fisher, I. R., Hussain, Z. and Shen, Z.-X., "Experimental realization of a three-dimensional topological insulator, Bi_2Te_3 ," *Science* 325, 178-181 (2009).
- [7] Zhang, Tong, Cheng, Peng, Chen, Xi, Jia, Jin-Feng, Ma, Xucun, He, Ke, Wang, Lili, Zhang, Haijun, Dai, Xi, Fang, Zhong, Xie, Xincheng and Xue, Qi-Kun, "Experimental demonstration of topological surface states protected by time-reversal symmetry," *Phys. Rev. Lett.* 103, 266803 (2009).
- [8] Roushan, P., Seo, J., Parker, C. V., Hor, Y. S., Hsieh, D., Qian, D., Richardella, A., Hasan, M. Z., Cava, R. J. and Yazdani, A., "Topological surface states protected from backscattering by chiral spin texture," *Nature (London)* 460, 1106-1110 (2009).
- [9] Alpichshev, Zhanybek, Analytis, J. G., Chu, J.-H., Fisher, I. R., Chen, Y. L., Shen, Z. X., Fang, A., and Kapitulnik, A., "STM imaging of electronic waves on the surface of Bi_2Te_3 : topologically protected surface states and hexagonal warping effects," *Phys. Rev. Lett.* 104, 016401 (2010).
- [10] Kim, Sunghun, Ye, M., Kuroda, K., Yamada, Y., Krasovskii, E. E., Chulkov, E. V., Miyamoto, K., Nakatake, M., Okuda, T., Ueda, Y., Shimada, K., Taniguchi, M. and Kimura, A., "Surface scattering via bulk continuum states in the 3D topological insulator Bi_2Se_3 ," *Phys. Rev. Lett.* 107, 056803 (2011).
- [11] Checkelsky, J. G., Hor, Y. S., Cava, R. J. and Ong, N. P., "Bulk band gap and surface state conduction observed in voltage-tuned crystals of the topological insulator Bi_2Se_3 ," *Phys. Rev. Lett.* 106, 196801 (2011).
- [12] Steinburg, H., Gardner, D. R., Lee, Y. S. and Jarillo-Herrero, P., "Surface state transport and ambipolar electric field effect in Bi_2Se_3 nanodevices," *Nano Lett.* 10, 5032-5036 (2010).
- [13] Kim, D. H., Cho, S. J., Butch, N. P., Syers, P., Kirshenbaum, K., Adam, S., Paglione, J. and Fuhrer, M. S., "Surface conduction of topological Dirac electrons in bulk insulating Bi_2Se_3 ," *Nat. Phys.* 8, 459-463 (2012).
- [14] Taskin, A. A., Sasaki, S., Segawa, K. and Ando, Y., "Manifestation of topological protection in transport properties of epitaxial Bi_2Se_3 thin films," *Phys. Rev. Lett.* 109, 066803 (2012).
- [15] Hor, Y. S., Williams, A. J., Checkelsky, J. G., Roushan, P., Seo, J., Xu, Q., Zandbergen, H. W., Yazdani, A., Ong, N. P. and Cava, R. J., "Superconductivity in $\text{Cu}_x\text{Bi}_2\text{Se}_3$ and its implications for pairing in the undoped topological insulator," *Phys. Rev. Lett.* 104, 057001 (2010).
- [16] Hor, Y. S., Roushan, P., Beidenkopf, H., Seo, J., Qu, D., Checkelsky, J. G., Wray, L. A., Hsieh, D., Xia, Y., Xu, S.-Y., Qian, D., Hasan, M. Z., Ong, N. P., Yazdani, A. and Cava, R. J., "Development of ferromagnetism in the doped topological insulator $\text{Bi}_{2-x}\text{Mn}_x\text{Te}_3$," *Phys. Rev. B* 81, 195203 (2010).
- [17] Schmidt, T. M., Miwa, R. H. and Fazzio, A., "Spin texture and magnetic anisotropy of Co impurities in Bi_2Se_3 topological insulators," *Phys. Rev. B* 84, 245418 (2011).
- [18] Yu, R., Zhang, W., Zhang, H.-J., Zhang, S. C., Dai, X. and Fang, Z., "Quantized anomalous hall effect in magnetic topological insulators," *Science* 329, 61-64 (2010).
- [19] Wray, L. A., Xu, S.-Y., Xia, Y., Hsieh, D., Fedorov, A. V., Hor, Y. S., Cava, R. J., Bansil, A., Lin, H. and Hasan, M. Z., "A topological insulator surface under strong Coulomb, magnetic and disorder perturbations," *Nat. Phys.* 7, 32-37 (2011).
- [20] Lind, Hanna, Lidin, Sven and Häussermann, Ulrich, "Structure and bonding properties of $(\text{Bi}_2\text{Se}_3)_m(\text{Bi})_n$ stacks by first-principles density functional theory," *Phys. Rev. B* 72, 184101 (2005).
- [21] Shih, H. C., Chen, L. Y., Luo, C. W., Wu, K. H., Lin, J.-Y., Juang, J. Y., Uen, T. M., Lee, J. M., Chen, J. M. and Kobayashi, T., "Ultrafast thermoelastic dynamics of HoMnO_3 single crystals derived from femtosecond optical pump-probe spectroscopy," *New J. Phys.* 13, 053003 (2011).

- [22] Luo, C. W., Wu, I. H., Cheng, P. C., Lin, J.-Y., Wu, K. H., Uen, T. M., Juang, J. Y., Kobayashi, T., Chareev, D. A., Volkova, O. S. and Vasiliev, A. N., "Quasiparticle dynamics and phonon softening in FeSe superconductors," *Phys. Rev. Lett.* 108, 257006 (2012).
- [23] Sobota, J. A., Yang, S., Analytis, J. G., Chen, Y. L., Fisher, I. R., Kirchmann, P. S. and Shen, Z.-X., "Ultrafast optical excitation of a persistent surface-state population in the topological insulator Bi_2Se_3 ," *Phys. Rev. Lett.* 108, 117403 (2012).
- [24] Wang, Y. H., Hsieh, D., Sie, E. J., Steinberg, H., Gardner, D. R., Lee, Y. S., Jarillo-Herrero, P. and Gedik, N., "Measurement of intrinsic Dirac fermion cooling on the surface of the topological insulator Bi_2Se_3 using time-resolved and angle-resolved photoemission spectroscopy," *Phys. Rev. Lett.* 109, 127401 (2012).
- [25] Chen, H.-J., Wu, K. H., Luo, C. W., Uen, T. M., Juang, J. Y., Lin, J.-Y., Kobayashi, T., Yang, H.-D., Sankar, R., Chou, F. C., Berger, H. and Liu, J. M., "Phonon dynamics in $\text{Cu}_x\text{Bi}_2\text{Se}_3$ ($x=0, 0.1, 0.125$) and Bi_2Se_2 crystals studied using femtosecond spectroscopy," *Appl. Phys. Lett.* 101, 121912 (2012).
- [26] Chis, V., Sklyadneva, I. Yu., Kokh, K. A., Volodin, V. A., Tereshchenko, O. E. and Chulkov, E. V., "Vibrations in binary and ternary topological insulators: first-principles calculations and Raman spectroscopy measurements," *Phys. Rev. B* 86, 174304 (2012).
- [27] Dantzig, N. A. van and Planken, P. C. M. "Time-resolved far-infrared reflectance of n-type GaAs," *Phys. Rev. B* 59, 1568 (1999).